

1N-34
394 823

**AN EXPERIMENTAL STUDY OF PRESSURE OSCILLATION IN A CAPILLARY PUMPED LOOP WITH
MULTIPLE EVAPORATORS AND CONDENSERS**

Jentung Ku
National Aeronautics and Space Administration
Goddard Space Flight Center
Greenbelt, Maryland
Tel: (301) 286-3130
Fax: (301) 286-1692

Triem T. Hoang
TTH Research, Inc.
Laurel, Maryland

33rd Intersociety Energy Conversion Engineering Conference
August 2-6, 1998, Colorado Springs, Colorado

AN EXPERIMENTAL STUDY OF PRESSURE OSCILLATION IN A CAPILLARY PUMPED LOOP WITH MULTIPLE EVAPORATORS AND CONDENSERS

Jentung Ku

National Aeronautics and Space Administration
Goddard Space Flight Center
Greenbelt, Maryland

Triem T. Hoang

TTH Research, Inc.
Laurel, Maryland

ABSTRACT

The heat transport capability of a capillary pumped loop (CPL) is limited by the pressure drop that its evaporator wick can sustain. The pressure drop in a CPL is not constant even under seemingly steady operation, but rather exhibits an oscillatory behavior. A hydrodynamic theory based on a mass-spring-dashpot model was previously developed to predict the pressure oscillation in a CPL with a single evaporator and a single condenser. The theory states that the pressure oscillation is a function of physical dimensions of the CPL components and operating conditions. Experimental data agreed very well with theoretical predictions. The hydrodynamic stability theory has recently been extended to predict the pressure oscillations in CPLs with multiple evaporators and multiple condensers. Concurrently, an experimental study was conducted to verify the theory and to investigate the effects of various parameters on the pressure oscillation. Four evaporators with different wick properties were tested using a test loop containing two condenser plates. The test loop allowed the four evaporators to be tested in a single-pump, two-pump or four-pump configuration, and the two condenser plates to be plumbed either in parallel or in series. Test conditions included varying the power input, the reservoir set point temperature, the condenser sink temperature, and the flow resistance between the reservoir and the loop. Experimental results agreed well with theoretical predictions.

INTRODUCTION

A capillary pumped loop (CPL) is a two-phase heat transfer device which utilizes surface tension forces developed in a fine-pore wick to circulate the working fluid. It is capable of transporting large heat loads over long distances with small temperature differentials and no external pumping power requirements [1,2]. Over the past two decades, extensive ground tests and several flight experiments have been conducted, and the potential of CPLs as reliable and versatile thermal control systems for space applications has been demonstrated [3-6]. The CPL has been developed to a high state of technology readiness and is currently the baseline design of the thermal control system for the Earth Observing System (EOS-AM), MARS98 Surveyor and Hubble Space Telescope third servicing mission (HST SM3) [7-9].

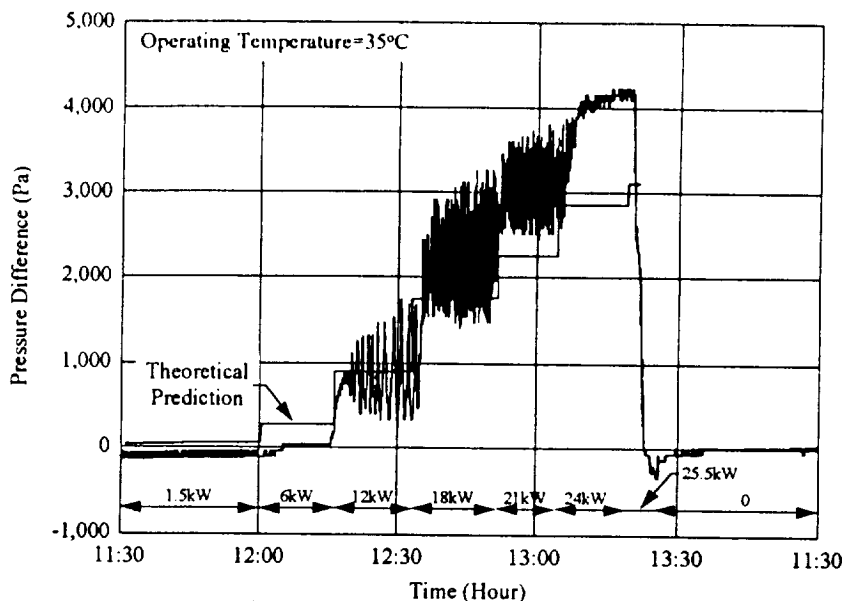


Figure 1. Pressure Oscillation in HPSTM

In CPL testing, a differential pressure transducer is usually used to measure the pressure drop across the evaporator in order to characterize the system performance. Figure 1 presents a typical differential pressure as a function of the heat input during ground testing of a CPL called High Power Spacecraft Thermal Management (HPSTM) system [10]. The pressure oscillation began at a power input of about 12 kW, and damped out near the system's heat transport limit of 24 kW. The pressure oscillation is not just a one-G phenomenon. Figure 2 depicts similar pressure oscillations for the Capillary Pumped Loop Flight Experiment (CAPL 2) onboard the Space Shuttle [6]. It can be seen that the pressure oscillation varied with the evaporator heat input and the condenser sink temperature. Other CPL systems also displayed oscillatory behaviors of the differential pressure. In most cases, the pressure oscillation did not appear to have any adverse effects on CPL operation. However, some CPL systems did exhibit performance anomalies [11], which might be related to the pressure oscillation. Specifically, the CPL could deprime when it was suddenly subjected to a large power decrease. A few years ago, a theoretical study based on the mass-spring-dashpot model was conducted in order to predict the hydrodynamic behavior and pressure oscillation in a CPL with a single evaporator and a single condenser [12]. Governing equations for a one-dimensional CPL fluid flow were derived based on conservation laws of mass, momentum and energy, and were expressed in terms of system mass flow rate, frictional and dynamic pressure drops, and vapor volumes in the vapor line and reservoir. The theory states that the pressure oscillation is a result of certain disturbance in the CPL. Under certain conditions, a small disturbance entering the system can acquire energy from the system and grow to a magnitude that it completely changes the equilibrium state of the system. Yet, under other conditions, the same disturbance may remain small or be damped out, leaving the equilibrium state unchanged. The frequency and amplitude of the pressure oscillation are functions of physical properties of the CPL components such as wick permeability, transport line sizes and vapor volumes, and operating conditions such as the power input and condenser sink temperature. Experimental data agreed very well with theoretical predictions [13].

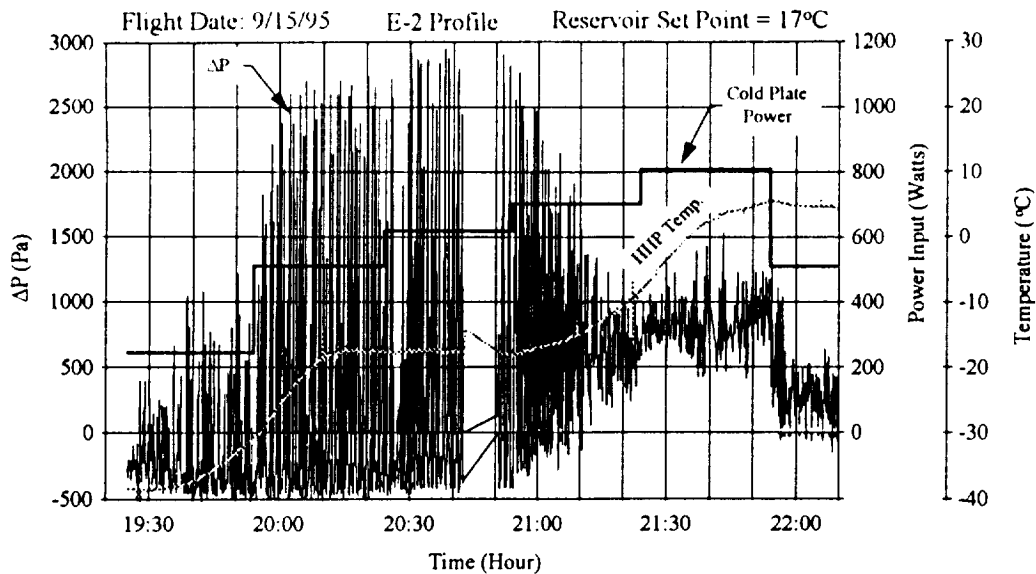


Figure 2. Pressure Oscillations in CAPL 2 Flight Experiment

Since many applications require CPLs to have multiple evaporators and multiple condensers, it is necessary to expand the existing CPL hydrodynamics stability theory to model such systems. An upgraded model capable of predicting pressure oscillations for multi-evaporator, multi-condenser CPLs has recently been developed [14]. Equations governing the overall thermal and hydraulic behaviors of the loop are very similar to those for single-evaporator, single-condenser CPLs. However, additional governing equations are needed for the evaporator and condenser sections such that conservation laws of mass, momentum, and energy are satisfied within these sections. Other features of the expanded hydrodynamic stability theory include: 1) an empirical correlation yielding the wick spring constant as a function of pore size, permeability and porosity; 2) nonlinear behaviors of the CPL fluid dynamics (e.g. turbulent pressure drop); 3) the degradation of heat transfer coefficient in the evaporator due to power increase as a source of disturbance; and 4) the capillary back pressure exerted on the vapor side of the loop by capillary devices such as condenser flow regulators.

The objectives of this experimental study were to: 1) verify the expanded CPL hydrodynamic stability theory [14]; and 2) study effects of various system parameters and operating conditions on the pressure oscillation. Details of the test program are described in the following sections. Test results and their implications on the design and operation of CPLs are also discussed.

PRESSURE DROPS IN A CPL

To help understand the phenomenon of pressure oscillation in a CPL, a brief review of physical processes involved in the CPL operation is presented. When a CPL is operational, the menisci formed at the liquid/vapor interface in the wick will curve naturally so as to provide the necessary capillary pressure rise that matches the total system pressure drop in the loop. For a CPL with only one evaporator and one condenser, the total pressure drop is the sum of the pressure drops in individual components along the flow path. If multiple, parallel condensers are present, the mass flow must be distributed among all condensers in such a way that conservation

laws of mass, momentum, and energy are satisfied within the condenser section. The flow distribution is a function of the line size and sink temperature of each individual condenser, and the plumbing arrangement. The total pressure drop across the condenser section is the difference of the pressures at the inlet and the outlet of the condenser assembly. For multiple, parallel evaporators, the mass flow rate through each evaporator is determined by the externally imposed heat load to that evaporator, independent of flow rates of other evaporators. Unlike in multiple condensers, the pressure drops play no role in determining the flow distribution among parallel evaporators. In other words, heat loads alone determine the flow rates in all evaporators. Once the flow rates through all evaporators are established, each wick must develop appropriate capillary force to balance the pressure drops among all evaporators. The pressure drop across the evaporator section, measured between the liquid inlet and vapor outlet of the evaporator assembly, is a function of the total heat loads to all evaporators, and this pressure drop is imposed upon all evaporators, even for those evaporators receiving no net heat input. Each evaporator is further subjected to an additional internal pressure drop as fluid flows through liquid channel inside the wick, the wick, and vapor grooves. The higher the heat load to an evaporator, the higher the internal pressure drop, and the more the menisci have to curve. Therefore, the vapor volume that is displaced into the wick of each evaporator depends upon the total heat load as well as the heat load to that evaporator. The net result is that all pressure drops in the evaporator section are balanced and there is only one pressure drop across the entire evaporator assembly.

The wick spring constant is defined as the ratio of the pressure drop across the meniscus divided by the vapor volume displaced into the wick. Since the vapor volume displaced into the wick is not directly proportion to the pressure drop, the spring “constant” actually varies with the pressure drop. A wick with a larger spring constant is stiffer, and needs to curve less than the wick with a smaller spring constant when subjected to the same pressure drop. For a multi-evaporator CPL, each evaporator wick will develop its own spring constant in accordance with the power distribution such that the pressure drops in the evaporator section are balanced at any instant. The pressure oscillation describes the deviation of the pressure drop from its mean value. It is caused by a disturbance introduced into the loop. The disturbance causes the vapor volume in the loop (vapor in the evaporator grooves, vapor line and condenser) to expand or contract, deviating from its mean value. As the vapor volume in the loop fluctuates, so does the pressure drop. The effect of the loop vapor volume change on the pressure drop is further amplified by the expansion and contraction of vapor inside the reservoir. The amplification is transmitted to the loop through the reservoir feed line. An increase of the flow impedance (dynamic, or frictional, or both) in the reservoir feed line can alleviate the amplification effect of the reservoir. When the reservoir is completely filled with liquid or physically isolated from the rest of the loop, there is no amplification effect, and the disturbance will not grow. This is why a CPL operating in a constant conductance mode is always stable.

The vapor volume change in the loop can be divided into two parts: one that goes to the evaporators and one that goes to the condensers, although they are interdependent. If there is only one evaporator and one condenser, the single evaporator and the single condenser must accommodate their respective portion of the vapor volume change. When there are multiple evaporators and/or multiple condensers, those changes are shared among the peers. Thus, the presence of additional evaporators and/or condensers always makes the pressure oscillation smaller provided other conditions remain the same. Since the vapor volume displaced into each

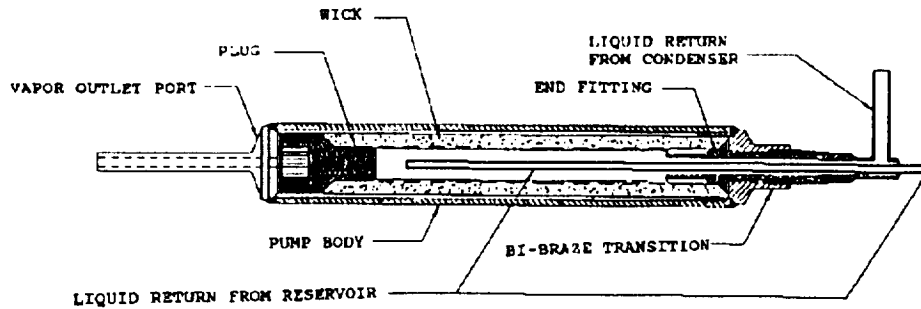


Figure 3. Schematic of Capillary Starter Pump

wick is a function of the total heat load to the evaporator section and the heat load into that evaporator, the pressure oscillation is also a function of the power distribution among all evaporators. Furthermore, the evaporator with the highest heat load will have the most influence in determining the system pressure oscillation.

TEST ARTICLES AND TEST LOOP

Four capillary starter pumps were used in this experimental study. These pumps are the development units for the EOS-AM program, and hence have a high fidelity to those used for thermal control of EOS-AM instruments. Figure 3 depicts a cross-sectional view of the starter pump. The pump body was made of aluminum extrusion with trapezoidal axial grooves (TAG-54) on the inner surface. Each pump had an active length of 559 mm (22 in.) and a nominal outer diameter (O.D.) of 30.5 mm (1.2 in.). A 3.18-mm (0.125 in.) O.D. stainless steel bayonet tube was inserted into the liquid channel of each pump. The wick was made of ultra high molecular weight polyethylene with a void volume of 50 percent. Important wick properties are presented in Table 1. All tests were conducted utilizing the Advanced Thermal System Testbed (ATST) at NASA Goddard Space Flight Center. The layout of the ATST is shown in Figure 4.

Table 1. Wick Properties

Pump No.	Serial No.	Wick Pore Size (μm)	Capillary Pressure Head (Pa/psi)	Wick Permeability ($\text{m}^2 \times 10^{13}$)
EVAP 1	SN103	8.35	4688/0.68	1.61
EVAP 2	SN105	8.0	4895/0.71	0.98
EVAP 3	SN023	15.5	2551/0.37	6.1
EVAP 4	SN010	14.4	2758/0.40	4.83

The test loop consisted of an evaporator section, a condenser section, a vapor line, a liquid line, and two reservoirs. The evaporator section could be configured to accommodate a single starter pump or up to four starter pumps. Two condenser cold plates of identical design were installed side by side. Each condenser plate consisted of three 7.94 mm O.D. x 0.89 mm W (5/16 in. x 0.035 in.) stainless steel condenser tubes, and each tube was serpentine into three passes for

a total active length of 1.83 m (72 in.). These tubes were imbedded and welded into the condenser plates. In one condenser, the three tubes were plumbed in parallel. In the other, two tubes were plumbed in series for a total condenser length of 3.66 m (144 in.) and the third tube was not used. Two hand valves were installed on the vapor manifold near the inlet of the condensers so that either or both condensers could be used at a time. The condensers were cooled by refrigerated coolant which flowed through another set of imbedded channels inside the condenser plate and ran perpendicular to the condenser tubes. Both the vapor and liquid lines were made of stainless steel tubing. The vapor line had a dimension of 9.53 mm O.D. x 0.89 mm W x 3.25 m L (0.375 in. x 0.035 in. x 127 in.), and the liquid line 6.35 mm O.D. x 0.89 mm W x 2.3 m L (0.250 in. x 0.035 in. x 91 in.). The space between adjacent evaporators was 230 mm (9.25 in.). There were two reservoirs in the loop; both were made of stainless steel. The first reservoir had an internal volume of 2.25 liters, and was used in this test program. The second reservoir had an internal volume of 1.0 liter and was intended for future tests. The reservoir feed line was made of stainless steel with a dimension of 6.35 mm O.D. x 0.71 mm W x 3.48 m L (0.25 in. x 0.028 in. x 137 in.). A hand valve was installed on the reservoir feed line. The opening of the valve was adjusted during the tests to provide variable flow resistances. At the evaporator section, the feed line formed a manifold and fed into each individual evaporator via a 508 mm (20 in.) feed line. The liquid return line was connected to the bayonet tube while the reservoir feed line was connected to the annulus of liquid channel inside the evaporator pump.

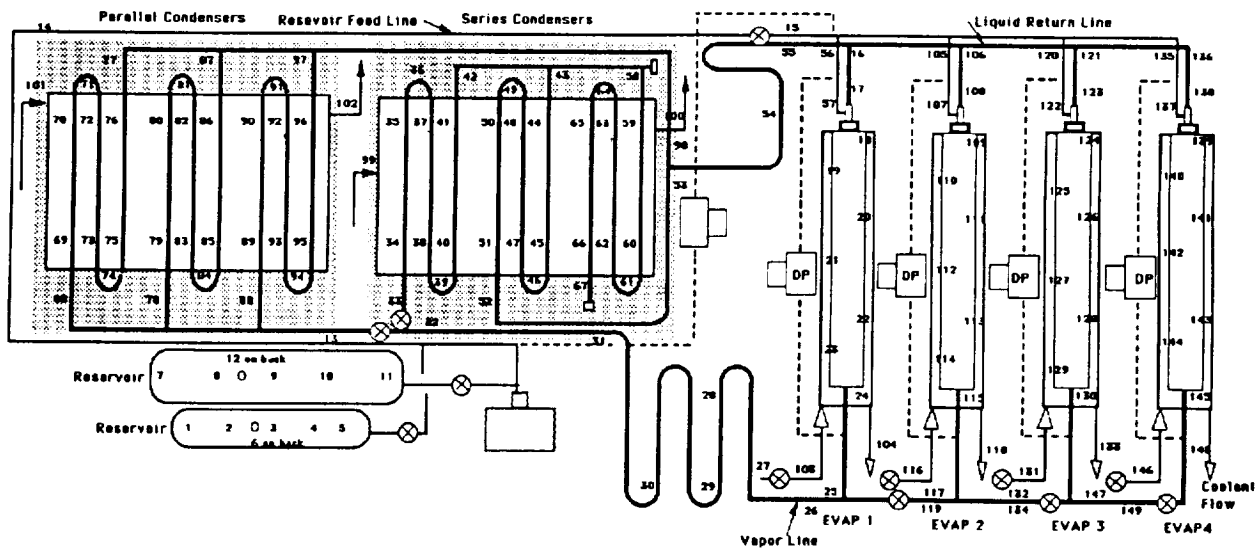


Figure 4. Schematic of the ATST Testbed

Each evaporator pump was sandwiched by two 76.2 mm x 559 mm x 12.7 mm thick (3 in. x 22 in. x 0.5 in.) aluminum blocks. Both aluminum blocks had electrical heaters attached, and the bottom block also contained flow channels through which liquid coolant was circulated during the heat load sharing test. Electrical heaters were also installed on the outer surface of the reservoir to control its set point temperature. A 15-kW refrigerator was used to provide cooling for the condensers at all times, and to the evaporator bottom blocks during heat load sharing tests. A pressure transducer was installed on the reservoir feed line to measure the absolute pressure of the loop. Five differential pressure transducers were installed: one across the reservoir feed line,

and one across each of the four evaporators. One hundred fifty type T thermocouples were used to monitor system temperatures at various locations. The entire loop was insulated with 12.7 mm-thick (0.5 in.) Armaflex insulation.

Test data was collected using a computerized data acquisition system, which consisted of a datalogger, a personal computer and a screen monitor. The data was updated and stored in the computer every 3 seconds. In addition, three strip chart recorders were employed for instantaneous display of the five differential pressures.

TEST PROGRAM

Tests were first conducted under the single-pump configuration to establish a baseline for comparison. This was followed by tests in two-pump and four-pump configurations. Because of the time constraint, only pumps SN105 and SN103 were tested in single-pump and two-pump configurations.

According to the hydrodynamic stability theory, the following parameters will affect the pressure oscillation: power input to the evaporators, temperature difference between the reservoir and the condenser sink, vapor line diameter and length, liquid line diameter and length, reservoir feed line diameter and length, wick properties, number of evaporators, and number of condensers. For the current test program, the size and diameter of each fluid line were fixed, and the following parameters were changed: 1) power input: up to 1000 watts per evaporator; 2) reservoir set point: 25 °C or 35 °C; 3) condenser sink temperature: 0 °C, 10 °C, or 20 °C; 4) one, two or four evaporators in the evaporator section; 5) four wicks with different properties; 6) three parallel condensers or two series condensers; and 7) flow resistance across the reservoir feed line.

Tests were performed by changing one parameter at a time. Series condensers were first selected, and the valve on the vapor line leading to the parallel condensers was closed. The condenser sink temperature was maintained constant by running the refrigerator at a fixed set point temperature. After the loop was successfully started, power inputs to the evaporators were increased in steps. Typical power increments were 100 watts per evaporator. At each power level, the flow resistance in the reservoir feed line was changed by adjusting the valve opening. Four valve settings were used: 1/16 turn, 1/8 turn and ¼ turn open from the fully closed position, and fully open. After the high power was reached, tests were repeated by setting the condenser sink to another temperature. The same tests were then performed with parallel condensers. The majority of the tests were conducted with a reservoir set point of 25 °C, and a few tests were repeated at 35 °C set point.

The aforementioned tests were conducted in all test configurations. In the two-pump and four-pump configurations, additional tests were performed: 1) uneven power inputs to the evaporators with the power profile varying with time; 2) heat load sharing among evaporators, i.e. heat was applied to some evaporators while a coolant flow was circulated to other evaporators which received no heat input; and 3) heat was applied to some evaporators while the other evaporators remained idle with neither heat input nor coolant circulation.

TEST RESULTS

Test results in the single-pump, two-pump, and four-pump configurations are described below.

SINGLE-PUMP CONFIGURATION

Only two starter pumps, SN105 and pump SN103, were tested in the single-pump configuration. As shown in Table 1, the wick properties of these pumps are very similar. Both pumps had a very high capillary pumping head, however, they also had a low permeability and hence a high flow resistance. The wick spring constant can be calculated as a function of the pressure drop, wick pore size and permeability using the model developed in the hydrodynamic stability theory [14]. Figure 5 shows such a relationship for pumps SN103 and SN105. Since the system pressure oscillation is a strong function of the wick spring constant under the same conditions (set point, sink temperature, power input), it can be expected that the stability characteristics of the ATST in the single-pump configuration with these two pumps will be similar. Figures 6 and 7 indeed show similar pressure oscillations when these pumps were tested in the single-pump configuration.

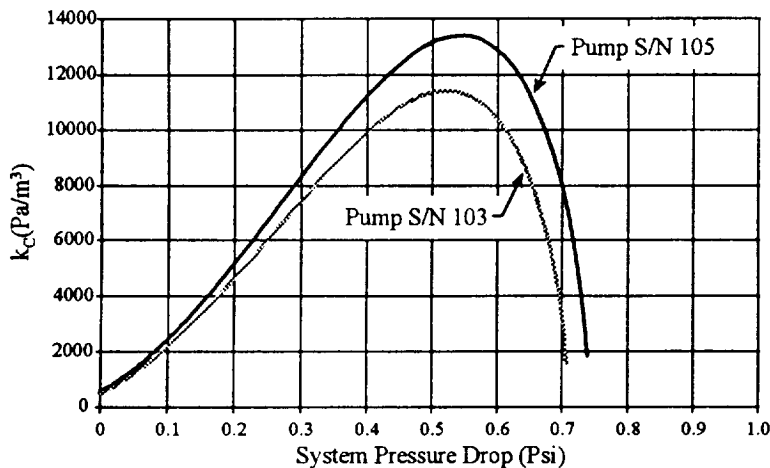


Figure 5. Spring Constants for Pumps SN103 and SN105

The predictions of the pressure oscillation for the parallel condensers compared very well with the test data for both pumps. However the predictions for the series condensers are not as good. The discrepancy was probably due to the fact that the current frictional pressure drop was calculated using a correlation based on the single-phase (all vapor) formulation in the vapor condensing zone of the condenser. Two-phase pressure drops in the condenser is usually 30-50% higher than their single-phase counterparts. For the ATST parallel condensers, the effect of two-phase flow was negligible because the pressure drop in the parallel condensers is small. When the computer model is incorporated into SINDA85/FLUINT [15] in the future, built-in two-phase pressure drop models (e.g. Lockhart-Martinelli) of FLUINT can be used to yield more accurate pressure drop in the condenser section. Therefore better predictions of the pressure oscillation are expected with the upgrade of the computer code.

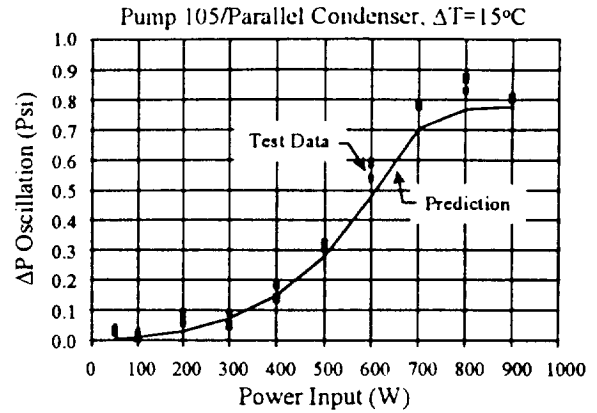
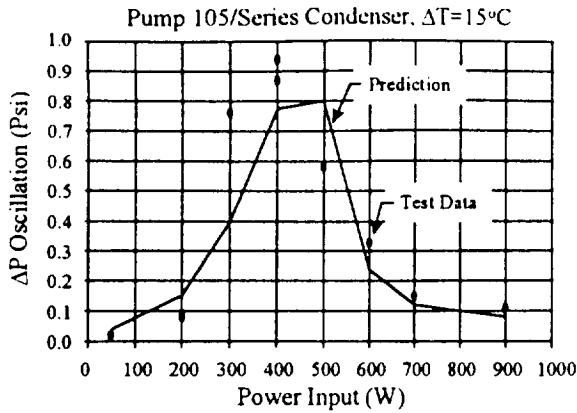


Figure 6 - Single-Pump Tests with Pump SN105

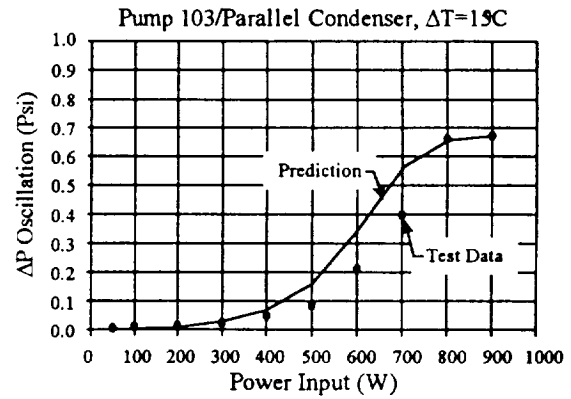
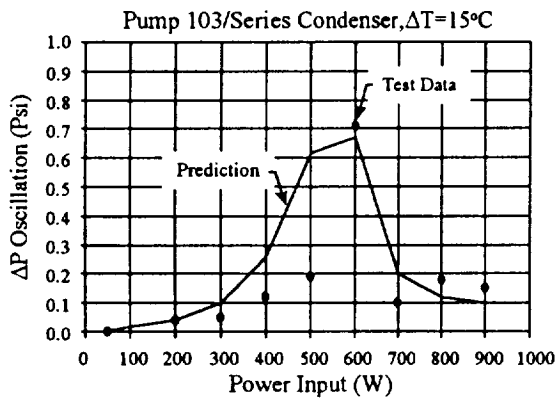


Figure 7 - Single-Pump Tests with Pump SN103

TWO-PUMP CONFIGURATION

Pumps SN105 and SN103 were used in the two-pump configuration. According to the hydrodynamic stability theory, the pressure oscillation in a two-pump configuration is a function of the spring constant of the two evaporator wicks, weighted by the flow rates through the evaporators. Since the wick properties of these pumps are very similar, however, the system pressure oscillation is primarily a function of the total system power. In other words, in this particular case, the power distribution between the two pumps has only a secondary effect on the pressure oscillation. Figures 8 and 9 shows the correlation between the analytical predictions and experimental data for the two-pump configuration with parallel and series condensers, respectively. It is seen in Figure 8 that the pressure oscillations are very similar with even or uneven heating at total heat loads of 100 watts, 200 watts, 400 watts, and 1000 watts when parallel condensers were used. Similar characteristic was seen in Figure 9 with total heat loads of 100 watts, 200 watts, and 400 watts when series condensers were used.

Figure 9 also shows the two-pump test data where pump SN103 was idle and all the heat load was applied to pump SN105. It can be seen that in this case the pressure oscillation was smaller than that in the single-pump test shown in Figure 6 with the same heat loads up to 400 watts. For heat loads of 500 watts or higher, it appears that the spring constant of pump SN105 reached its maximum and dropped sharply with an increasing pressure drop. Any factors affecting the total pressure drop will also impact the spring constant and the pressure oscillation, and the comparison between Figure 9 and Figure 6 becomes more difficult.

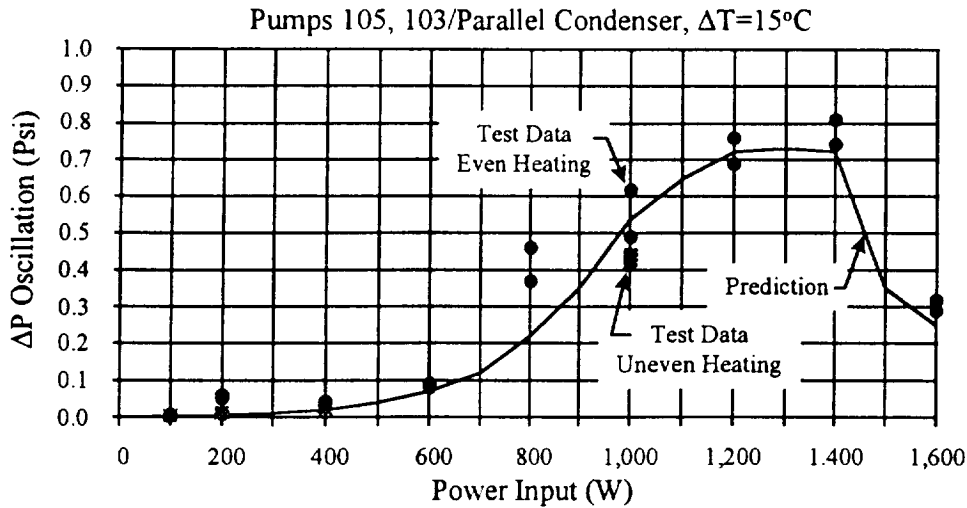


Figure 8. Two-Pump Tests with Pumps SN105 and SN103 and Parallel Condensers

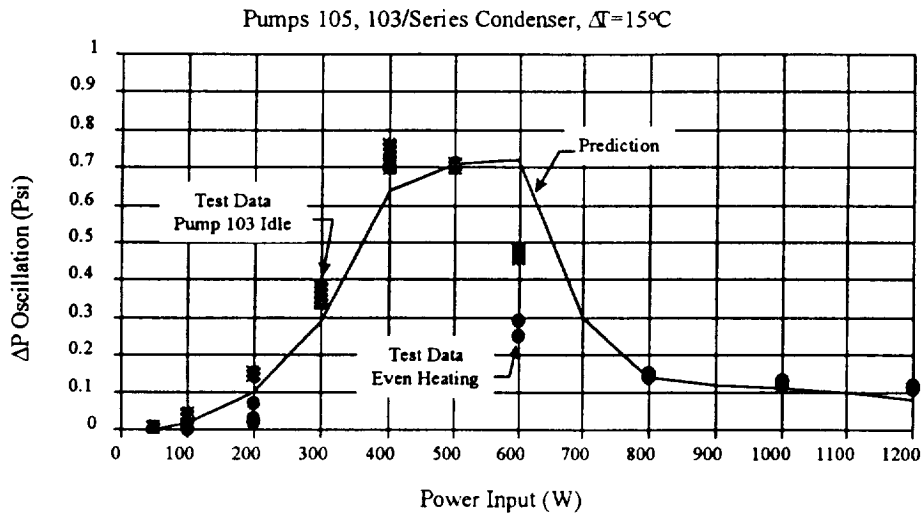


Figure 9. Two-Pump Tests with Pumps SN105 and SN103 with Series Condensers

FOUR PUMP CONFIGURATION

Table 1 shows that Pumps SN105 and SN103 have similar wick properties, and so do Pumps SN023 and SN010. However, these two groups have drastically different pore sizes and

wick permeabilities. Since the pressure oscillation is a function of the spring constant of the evaporator wicks, weighted by flow rates through these evaporators, it is expected that the pressure oscillation will be strongly dependent upon the power distribution among the four evaporators.

Figures 10 (a) and 10(b) shows the pressure oscillations in the four-pump configuration when series and parallel condensers were used, respectively. As the number of components increases, there are more uncertainties in the experimental conditions. Nevertheless, theoretical predictions agree fairly well with experimental data for the most part. Effects of various parameters on the pressure oscillation are discussed below.

Effect of Sink Temperature: The hydrodynamic stability theory predicts that the pressure oscillation will increase as the temperature difference between the reservoir set point and the condenser sink temperature increases. Figures 10(a) and 10(b) show that the pressure oscillation is always higher at a temperature difference of 35 °C than at 15 °C for any given power input. This is true for the full range of powers tested and for both series and parallel condensers.

Effect of Condenser Design: Typically, the wick spring constant initially increases with an increasing system pressure drop, reaches a maximum, and then decreases, as depicted in Figure 5. The power input affects the pressure oscillation through its impact on the system pressure drop. Since the parallel condensers offer a smaller pressure drop than the series condensers for the same power input, the spring constant and the pressure oscillation will reach their maxima at a lower power input when series condensers are used. For the same power input, parallel condensers yield a smaller pressure oscillation than the series condensers until the spring constant reaches its maximum. Figures 10(a) and 10(b) clearly demonstrated these phenomena. The same conclusion applies to the single-pump and two-pump tests.

Effect of Uneven Heating of Parallel Capillary Pumps: As mentioned before, in a multi-evaporator CPL, the evaporator with the highest heat load will have the most influence on the pressure oscillation. For the four pumps tested, pump SN105 has the highest spring constant, followed by pump SN103. Figure 11 shows the pressure oscillation as a function of the power

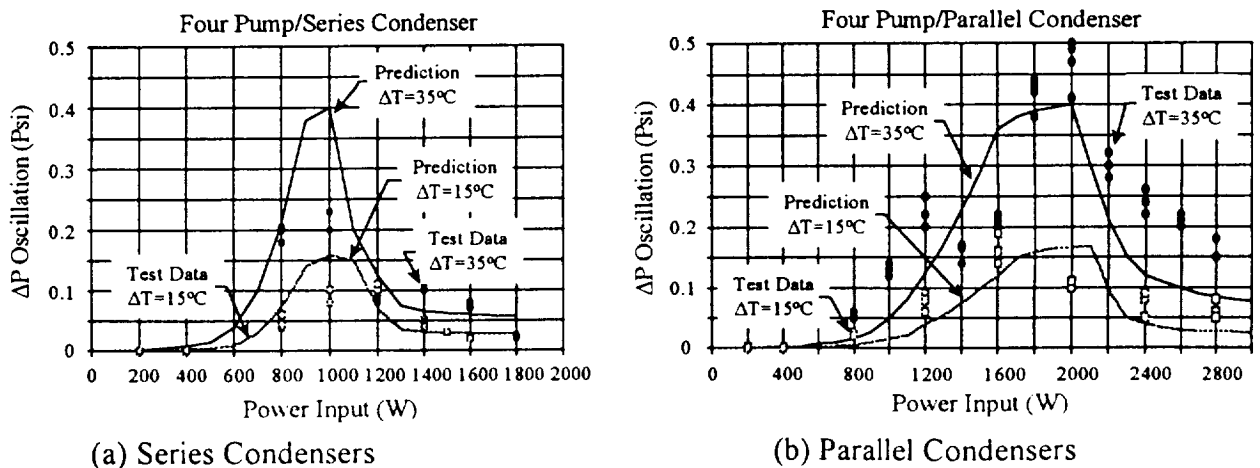


Figure 10. Four-Pump Tests

distribution among four pumps. It can be seen that whenever the power input to pump SN105 was 400 watts or higher, the pressure oscillation was high. When the power input to pump SN105 was low, then the power input to pump SN103 became the determining factor. By comparison, high power inputs to pumps SN023 and SN010 did not cause the pressure oscillation to increase because of their low wick spring constants.

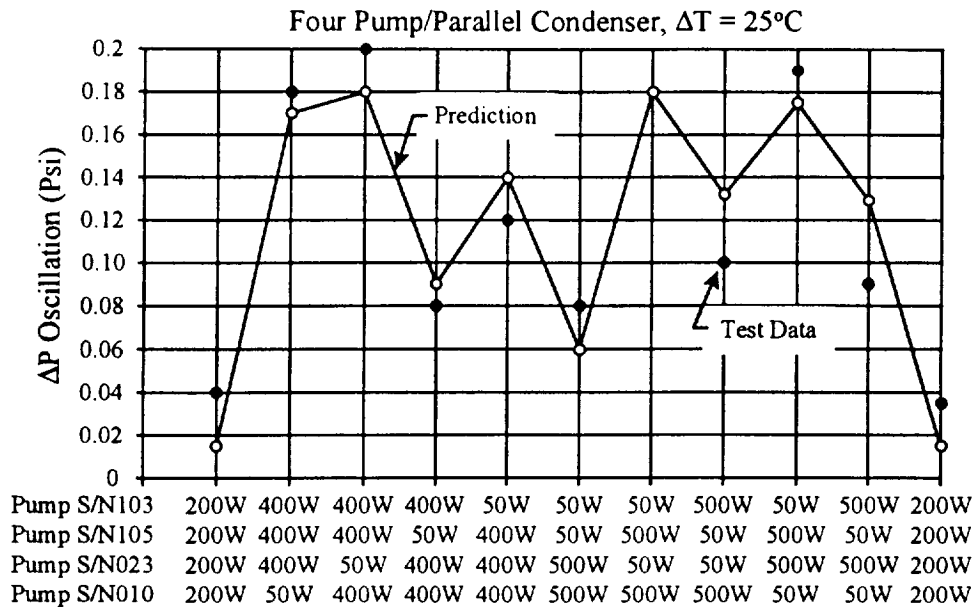


Figure 11 - Four-Pump Tests with Uneven Heating

Effect of Flow Resistance of Reservoir Feed Line: The flow resistance in the reservoir feed line connecting the main loop to the reservoir has a profound effect on the CPL system stability. According to the hydrodynamic stability theory, a higher flow resistance in the transport lines (including vapor, liquid and reservoir lines) increases the dissipation of disturbance energy, and therefore should enhance the system stability. However increasing the flow resistance in the vapor and liquid lines can be counterproductive since it will cause the system pressure to increase, which in turn causes the pressure oscillation to increase. A viable option to reduce the pressure oscillation is to increase the flow resistance in the reservoir feed lines. A high flow resistance in the reservoir feed line reduces the amplification effect of the vapor expansion and contraction in the reservoir. Its effectiveness has been demonstrated in the previous studies of the CPL hydrodynamic stability [12, 13].

In this test program, the hand valve placed on the reservoir feed line was adjusted to different openings so as to provide variable flow resistance. Four valve settings were used at each power level during the high power tests: fully open, 1/4 turn, 1/8 turn, and 1/16 turn open from the fully closed position. As illustrated in Figure 12, the pressure oscillation became increasingly smaller as the valve opening was further reduced.

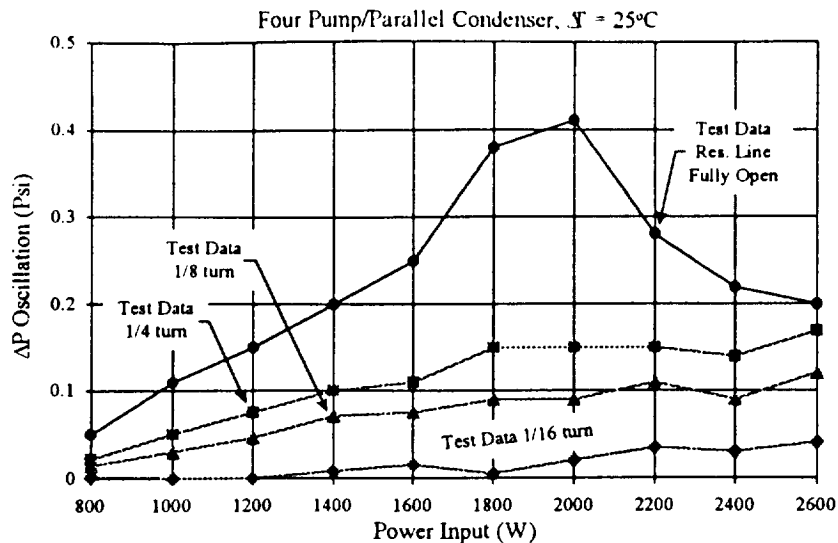


Figure 12 - Effects of Reservoir Line Resistance on Pressure Oscillations in Four-Pump Tests

CONCLUDING REMARKS

An experimental study of the pressure oscillation in a CPL with multiple evaporators and condensers was conducted in a test loop at NASA Goddard Space Flight Center. Test results verified that the pressure oscillation is a function of the wick properties, power input, flow resistance across the reservoir feed line, temperature difference between the loop and the condenser sink, and total system pressure drop. When multiple evaporators are present, the pressure oscillation is also dependent upon the power distribution among parallel evaporators. In general, theoretical predictions agreed fairly well with experimental data over a wide range of system operational conditions. The effects of individual parameters on the pressure oscillation are also correctly predicted and experimentally verified.

Pressure oscillations have been observed in all CPL systems equipped with differential pressure transducers. The pressure oscillation could have profound impacts on the system operation. In many systems, the evaporator deprived at heat loads well below its theoretical heat transport limit because the pressure drop at the peak of the oscillation exceeded its capillary limit. The ability to predict accurately the pressure oscillation in a CPL is therefore of vital importance to the operational success of the system. Furthermore, early detection of the stability problem at the design phase enables the CPL engineers to build a more reliable system without expensive and time-consuming testing.

This experimental study also suggests that CPL performance is a strong function of interactions between its components. A corollary to this statement is that components that work well in one CPL may show significantly different behaviors when tested in other CPLs. Thus, a system approach is needed for a proper CPL design. Traditional design approach taken in the early developments of CPLs, which only took into consideration the static pressure drop in sizing

the loop components, is no longer adequate. Rather, an optimization between the system heat transport limit, system start-up transient, and system pressure oscillation is needed. The following design procedure is recommended: 1) Size the CPL components for the required maximum heat transport based on steady operation without pressure oscillations. 2) Analyze the pressure surge during the start-up transient when the vapor line is being cleared of liquid. Make adjustments on transport line sizes, if necessary, to keep the pressure surge within the capillary limit. 3) Analyze the pressure oscillation based on the hydrodynamic stability theory to further characterize the system behavior. If the amplitude of the pressure oscillation exceeds the wick's capillary limit before the theoretical heat transport limit is reached, some adjustments on the components sizing are required. 4) Repeat the above steps until an optimal design is reached. The ultimate goal of the future development is the incorporation of the CPL hydrodynamic stability into a thermal/fluid analyzer such as SINDA85/FLUINT [15] so that a single thermal/hydraulic analyzer can be used for CPL design.

REFERENCES

1. Ku, J., "Overview of Capillary Pumped Loop Technology", 1993 ASME National Heat Transfer Conference, Atlanta, Georgia, 1993.
2. Cullimore, B., "Capillary Pumped Loop Application Guide", The 23rd International Conference on Environmental Systems, Colorado Springs, Colorado, 1993.
3. Ku, J., Kroliczek, J., Butler, D., Schweickart, R., and R. McIntosh, "Capillary Pumped Loop GAS and Hitchhiker Flight Experiments", AIAA Paper No. 86-1249, 1986.
4. Delil, A., Heemskerk, J., Dubois, M., van Oost, S., Supper, W., and R. Aceti, "In-Orbit Demonstration of Two-Phase Heat Transport Technology: TPX/G557 Flight Results", SAE Paper No. 941404, 1994.
5. Butler, D., Ottenstein, L., and J. Ku, "Flight Testing of the Capillary Pumped Loop Flight Experiment," SAE Paper No. 951566, 1995.
6. Ku, J., Ottenstein, L., and D. Butler, "Performance of CAPL 2 Flight Experiment," SAE Paper No. 961432, 1996.
7. Fredley, J. and A. Pelszynske, "Accommodation of the EOS AM Instrument Set Using Capillary Pumped Heat Transport Technology", SAE Paper No. 921404, 1992.
8. Clayton, S., Martin, D., and J. Baumann, "Mars Surveyor Thermal management Using a Fixed Conductance Capillary Pumped Loop," SAE paper 972467, 1997.
9. McIntosh, R., Kaylor, M., Buchko, M., Kroliczek, E., and B. Smith, "A Capillary Pump Loop Cooling System for the NICMOS Instrument," 28th International Conference on Environmental Systems, Danvers, Massachusetts, July 13-16, 1998.
10. Ku, J., Kroliczek, E. J., McCabe, M., and S. M. Benner, "A High Power Spacecraft Thermal Management System", AIAA Paper No. 88-2702, 1988.
11. Ottenstein, L., Ku, J., and D. Butler, "Thermal Vacuum Testing of the Capillary Pumped Loop Flight Experiment", SAE Paper No. 941599, 1994.
12. Hoang, T, and J. Ku, "Theory of Hydrodynamic Stability for Capillary Pumped Loops", ASME National Heat Transfer Conference, Portland, Oregon, 1995.
13. Ku, J. and T. Hoang, "An Experimental Study of Pressure Oscillation and Hydrodynamic Stability in a Capillary Pumped Loop", ASME National Heat Transfer Conference, Portland, Oregon, 1995.]

14. Hoang, T, and J. Ku, "Theory of Hydrodynamic Stability for Capillary Pumped Loops with Multiple Evaporators and Condensers", 33rd Intersociety Energy Conversion Engineering Conference, Colorado Springs, Colorado, August 2-5, 1998.
15. "SINDA85/Fluint: Systems Improved Numerical Differencing Analyzer and Fluid Integrator," Version 4.0, Cullimore and Ring Technologies, Inc., October, 1997.